Editor's Note: In Part III, the authors describe methods to reduce stiction effects in the capacitive (metal-insulator-metal) contact MEMS switch for applications in low SNR signal routing application in modern electronics circuits including 5G communication. Also, experimental results to validate simulation results presented earlier for DSG structure-based metamaterial switch are also included in this paper. As described in Part I (May Issue), the combination of a primary shunt switch, DGS structures and secondary shunt switches, is shown to behave like a metamaterial. In Part II, the authors have shown new ways to reduce stiction effects in the Resistive MEMS switch (metal-to-metal contact) using artificially created metamaterial structure.
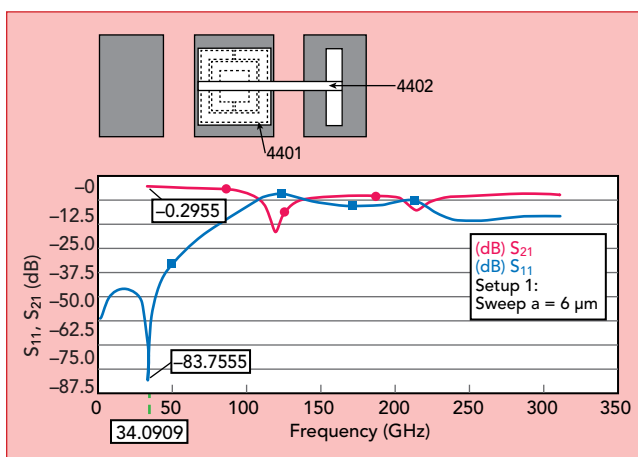
A Microelectromechanical Switch with Metamaterial Contacts, Part III: Reducing Stiction

Shiban K. Koul and Pranav K. Srivastava
C.A.R.E, Indian Institute of Technology, Delhi, India

Ajay K. Poddar and Ulrich L. Rohde
Synergy Microwave, N.J., U.S.

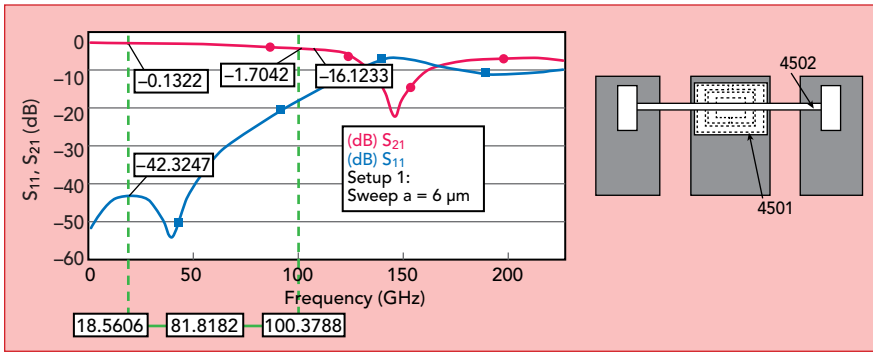The theory of a repulsive Casimir force and application in a resistive contact MEMS switch is discussed in detail in Part II (June Issue). In this article, a new method to reduce the stiction effects in the capacitive (metal-insulator-metal) contact MEMS switch that has applications in low SNR signal routing application in modern electronics circuits including 5G communication is described.[1-8] In addition, experimental results to validate simulated results presented earlier for DSG structure-based metamaterial switch are included.
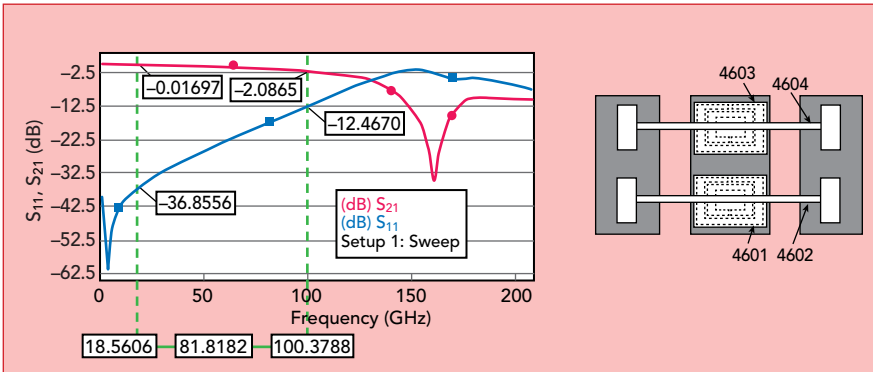
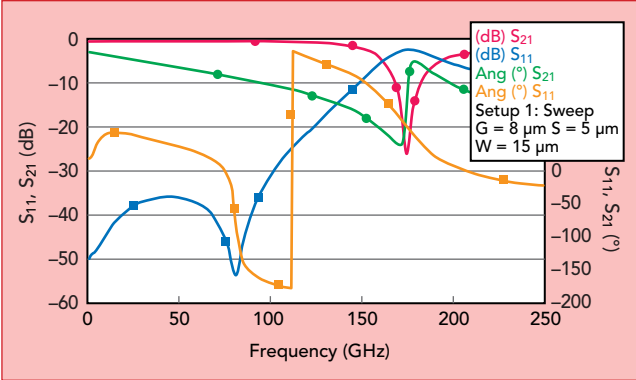## CASIMIR REPULSIVE FORCE INSPIRED CAPACITIVE MEMS SWITCH

The metamaterial unit cell described in reference[9] and realized using a composite engineered structure, provides promising characteristics in the relevant band of frequencies for the MEMS switch (e.g., between 60 to 130 GHz). **Figures 1** to **3** provide results for transmission and reflection characteristics for a respective unit cell structure. The composite structure, 4401 illustrated in Figure 1, is included in a metal layer

▲ **Fig. 1** Transmission and reflection characteristics of composite structure described by 4401 and 4402.

▲ Fig. 2 Transmission and reflection characteristics of composite structure described by 4501 and 4502.

▲ Fig. 3 Transmission and reflection characteristics of composite structure described by 4601 and 4602.
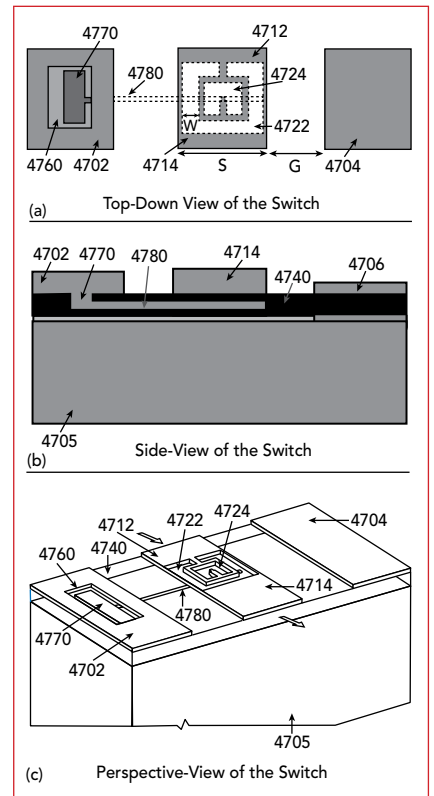

▲ Fig. 5 Transmission and reflection characteristics of capacitive MEMS switch in Figure 4.

▲ Fig. 4 Diagram of capacitive MEMS switch incorporating metamaterial cells to provide a repulsive Casimir Force between contacts of switch: (a) top-down view, (b) side view and (c) perspective view.

(e.g., of a signal line contact) and interfaces beam 4402. In this example, the beam is thinner than the metamaterial structure, and is supported by a single support extending from one of the ground planes adjacent the signal line. The unit cell is a transmission type at about 34 GHz (having reflection characteristics of -83.75 dB and transmission characteristics of -0.29 dB). The unit cell is a reflection type at about 120 GHz. Thus, the composite structure in Figure 1 is shown to exhibit metamaterial properties, can be used for

the realization of stiction free capacitive (metal-insulator-metal) contact MEMS switch.

The composite structure (4501) shown in Figure 2 is included in a metal layer (e.g., of a signal line contact) and interfaces with beam 4502. In this example, the beam is thinner than the metamaterial structure, and is doubly supported by posts on either side of the signal line. The unit cell is a transmission type at about 40 GHz (having reflection characteristics of -54 dB and transmission characteristics of -0.5 dB). The unit cell is a reflection type at about 140 GHz. Thus, the structure of Figure 2 is shown to exhibit metamaterial properties also, hence can be used for the realization of stiction free capacitive (metal-insulator-metal) contact MEMS switch.
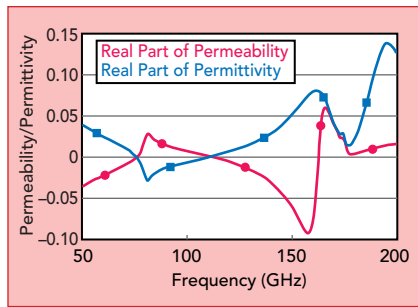
Figure 3 includes two composite structures, 4601 and 4603, posi-

tioned at opposing input and output sides of the signal line. Each composite structure is included in a metal layer (e.g., of the signal line contact). Further, doubly supported beams, 4602 and 4604, are positioned above each of the composite structures. As in the example of Figure 2, the beams are thinner than the metamaterial structures. The unit cell is a transmission type at about 8 GHz (having reflection characteristics of -60 dB and transmission characteristics of -0.01 dB). The unit cell is a reflection type at about 160 GHz. Thus, the structure of Figure 3 is shown to exhibit metamaterial properties too, hence can be used for the realization of stiction free capacitive (metal-insulator-metal) contact MEMS switch.

Another example of a capacitive MEMS switch is shown in **Figure 4**. As illustrated in Figure 4, the switch includes a structure formed over a signal line having an input side 4712 and an output side 4714. A metamaterial structure having an outer split ring 4722 and inner split ring 4724
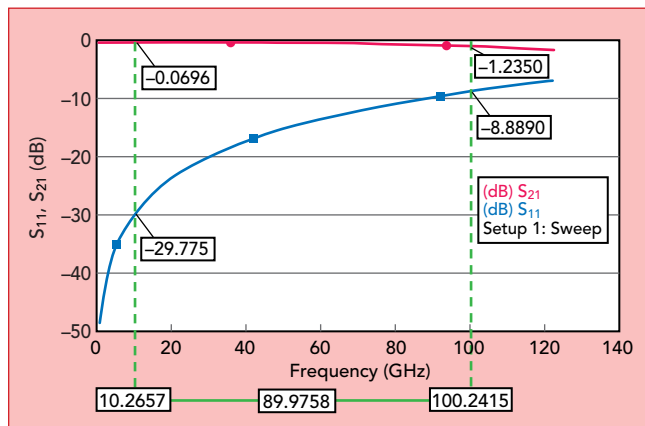
▲ Fig. 6 Plot of permittivity extracted from the S-parameters of the composite structure shown in Figure 4.
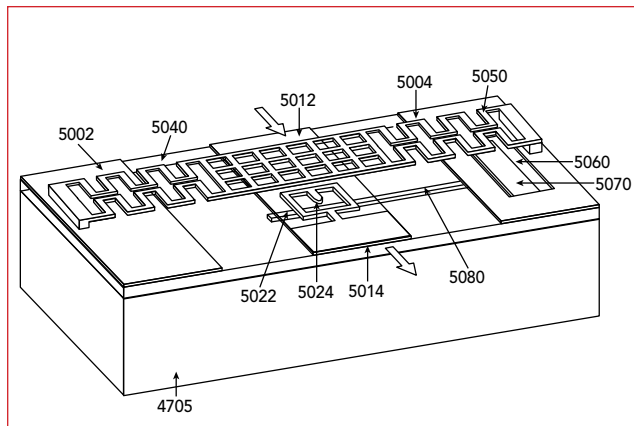
is formed in the signal line contact between the input side 4712 and output side 4714, through which a signal is received (arrow in) and an output port through which the signal is transmitted (arrow out).

Each of the ground planes 4702, 4704 and the signal line are formed from a conductive material, such as gold, and are formed on top of a dielectric material 4740 such as silicon nitride (Si3N4), which itself is formed on top of a substrate 4705. One of the ground planes 4702 includes a post 4770 extending downward from the ground plane 4702 into the dielectric material 4740, and a beam 4780 extending from the post 4770 in the direction of the signal line 4714. The edge of the beam 4780 is aligned with the opposing edge of the signal line 4712, 4714, such that the end of beam 4780 is positioned underneath the metamaterial structures 4722, 4724, of the signal line 4712, 4714. In Figures 4a and 4c, the post 4770 can be seen through an opening 4760 in the ground plane 4702.

In the example of Figure 4, the ground planes and the signal line

▲ Fig. 8 Transmission and reflection characteristics of capacitive MEMS switch shown in Figure 7 in the ON State.

▲ Fig. 7 Perspective view of a capacitive shunt MEMS switch utilizing a metamaterial signal line contact to reduce stiction in the switch.

may each have a width (in the direction of the beam 4780 length) of about 73 μm and the beam may have a length of about 168 μm. The metamaterial structure formed on the signal line contact may have a ring width W of about 15 μm, a split width G of about 8 μm and a spacing between rings S of about 5 μm.

Transmission and reflection characteristics of the switch over a range of frequencies are shown in **Figure 5**. The metamaterial is most reflective at about 175 GHz and most transmissive at about 80 GHz. Based on these results, material parameter extraction[10] can be performed to determine the permittivity and permeability of the metamaterial structure. The extraction of the permeability and permittivity are shown over a range of frequencies in **Figure 6**.

As seen in Figure 6, the metamaterial structure exhibits near zero permittivity and permeability between about 50 and 150 GHz. This indicates that the structure of Figure 4 is suitable for reducing the stiction using the Casimir force of interaction (repulsive) in the desired frequency band.
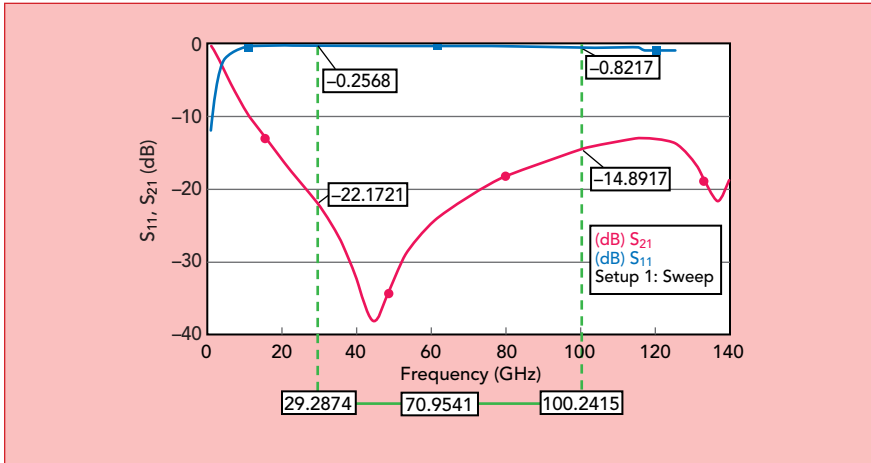
Figure 7 shows a perspective view of a capacitive shunt MEMS switch utilizing a metamaterial signal line contact

to reduce stiction in the switch. Many of the features of switch illustrated in Figure 7 may be compared to the switch described in Figure 4. The switch in Figure 7 also includes a deflectable beam 5050. The beam is comparable to the rectangular beam 510 described in connection wit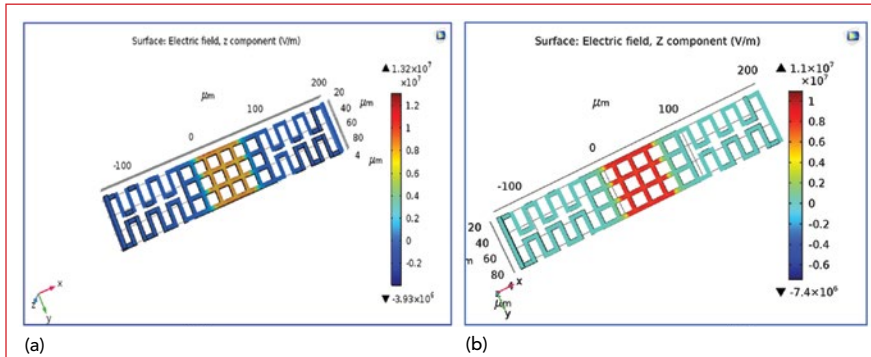h Figure 5 of Part I (May Issue) (e.g., may be made from gold, may have a perforated grid structure, may extend in a serpentine pattern). The deflectable beam 5050 is supported by a pair of posts formed on top of the ground planes 5002 and 5004, respectively, and is configured to deflect downward toward the signal line when actuated by a bias voltage.

In operation, the bias voltage causes the midpoint of the beam 5050 to deflect downward until it comes in contact with the signal line contact, thereby causing the signal line to turn off (or in other cases to turn on). When the bias voltage is removed, the midpoint of the beam 5050 deflects back upward. Because the midpoint of the beam is aligned with the metamaterial structure 5022, 5024 of the signal line contact, the Casimir effect at the interface between the beam and the signal line contact is diminished or even repulsive, thereby reducing the liability of stiction between the beam 5050 and the signal line.
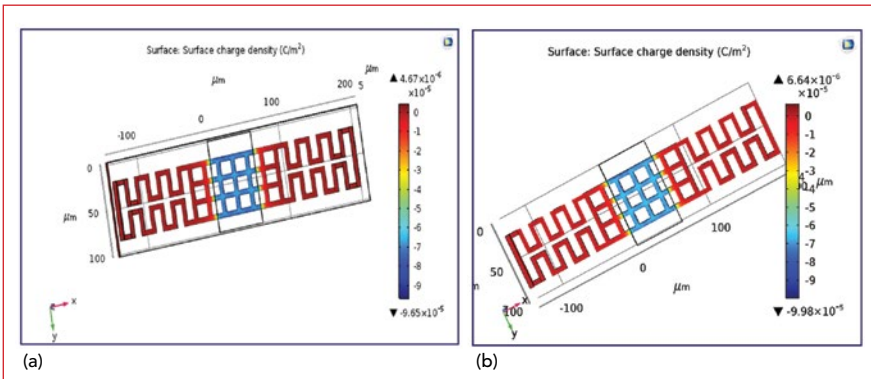
Although not shown in Figure 7, the signal line contact can include a layer of dielectric material above the metal layer including the metamaterial structure. The dielectric layer can function as an isolation layer to achieve the desired permittivity gradient, as discussed above in connection with Figure 5 (Part II, June Issue). In other words, the beam 5050 can have an infinite permittivity, the isolation layer can have a positive but smaller permittivity and the metal layer including the metamaterial structure in the signal line contact can have a near
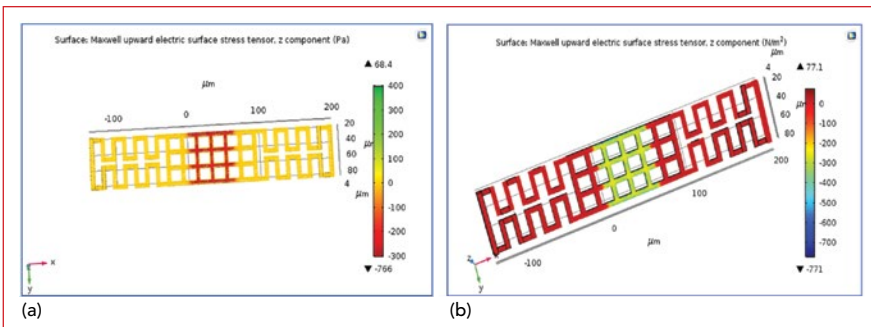
▲ **Fig. 9** Transmission and reflection characteristics of capacitive MEMS switch shown in Figure 7 in the OFF State.

▲ **Fig. 10** Electric field distribution of a shunt switch with serpentine signal line and (a) with and (b) without metamaterial.

▲ **Fig. 11** Surface charge density of a shunt switch with serpentine signal line and (a) with and (b) without metamaterial.

▲ **Fig. 12** Electric surface stress tensor of a shunt switch with serpentine signal line and (a) with and (b) without metamaterial.

zero, zero or negative permittivity, thereby satisfying $\varepsilon_1 < \varepsilon_2 < \varepsilon_3$ condition or vice-versa. The performance of the capacitive MEMS switch (Figure 7) is shown in **Figures 8** and **9** which are plots of the reflection and transmission characteristics of the switch across a range of high RF frequencies. Figure 8 demonstrates operation of the switch in the ON state (transmitting signals) and Figure 9 demonstrates operation of the switch in the OFF state (cutting off transmission of signals).

In Figure 8, most notably, at 10.3 GHz, return loss is as high as 29.8 dB while insertion loss is as low as about 0.07 dB. Even at 100.2 GHz, return loss is as high as 8.9 dB while insertion loss is only about 1.23 dB. This demonstrates good operation of the switch in the ON state across a wide range of high frequencies, from 10 to 100 GHz.

In Figure 9, the switch is OFF, thus changing to being reflective instead of transmissive. At 29.3 GHz, insertion loss is as high as about 22.2 dB while return loss is as low as about 0.26 dB. Even at 100.2 GHz, insertion loss is as high as 14.9 dB while return loss is only about 0.82 dB. This demonstrates good operation of the switch in its OFF state across nearly the same wide range of high frequencies, from about 20 to 100 GHz.

Good insertion loss and return loss characteristics of the MEMS switch in the ON and OFF states are achieved over 30 to 100 GHz. This makes the presently described switch a good candidate for high frequency switching operations over a wide bandwidth of frequencies. Accordingly, the switches described can improve operation and performance of applications requiring high frequencies over a wide bandwidth. Such technologies may include 5G communications, switching networks, phase shifters (e.g., in electronically scanned phase array antennas) and IoT applications.

CASIMIR FORCE STUDY

In Part I (May Issue), it is shown that a combination of a primary shunt switch, DGS structures and secondary shunt switches behave like a metamaterial. In Part II (June

Issue), improvement of resistance to stiction of the MEMS switch using metamaterial layers within the design of resistive switch contact is covered. Here in Part III, the metamaterial layers are used as part of the signal line contacts to realize capacitive switch to improve stiction and hence reliability.

To get more insight into the repulsive Casimir forces generated in these structures, a detailed study of a shunt switch with serpentine signal line with and without metamaterial underneath was carried out using COMSOL software. *Figures 10* to *12* show electric field distribution, surface charge distribution and electric surface stress tensor of a shunt switch with serpentine signal line with and without metamaterial underneath.
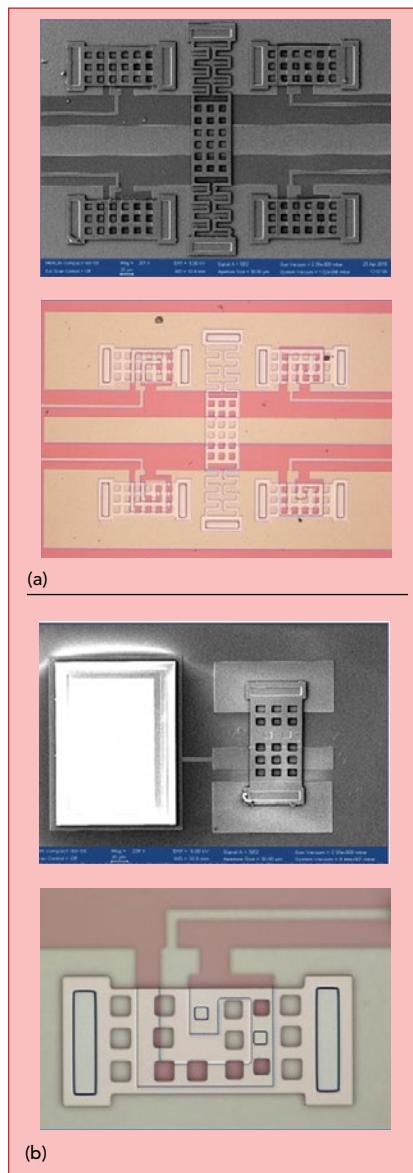
From these results, one can estimate Casimir force. The estimated Casimir force of a shunt switch with serpentine signal line with and without metamaterial underneath is shown in *Figure 13* and *Table 1* shows key parameters for the serpentine structure with and without the metamaterial. As observed, the structure with metamaterial underneath exhibits Casimir repulsive force.

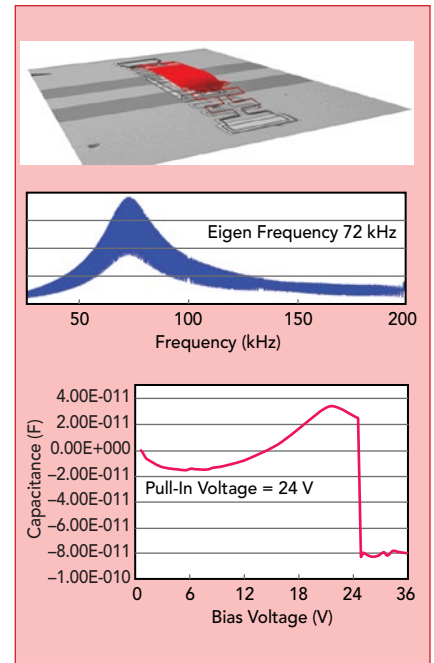To verify the accuracy of the simulations, sample structures were

(a)

(b)

▲ **Fig. 13** Estimated Casimir Force of a shunt switch with serpentine signal line and (a) with and (b) without metamaterial.

fabricated using the PolyMUMPs process and characterized. As an example, the metamaterial inspired MEMS shunt switch shown in Figure 15 (Part I, May Issue) was fabricated and characterized. The SEM and optical microscope images of the fabricated structure are shown in *Figure 14*. Both primary and secondary switches were experimentally characterized and Eigen frequency, CV characteristics, profiling and LDV plotted. It was observed that the results obtained from the simulations matched with measured data.

Figure 15 and *16* show the measured results (all the measurements

(a)

(b)

▲ **Fig. 14** SEM image and Optical Microscope images of (a) primary and (b) secondary shunt switches.
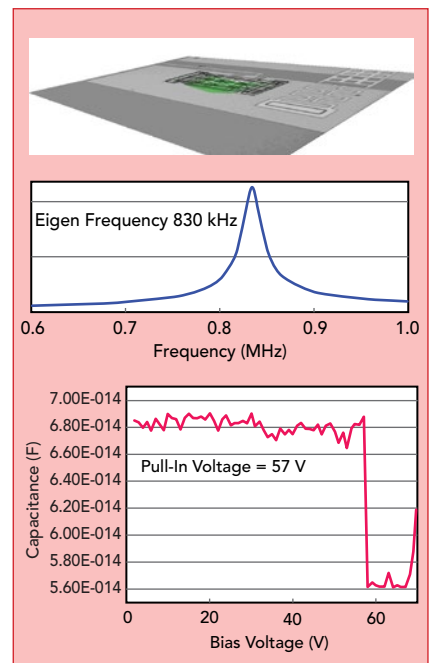
were done on bare die). It was observed that by using serpentine beam, pull in voltage reduced by 9 V. Work on different packages suitable for the present application was also done separately.[11-12] Using these techniques, measurements were carried out after packaging without noticing significant changes in the switch performance.
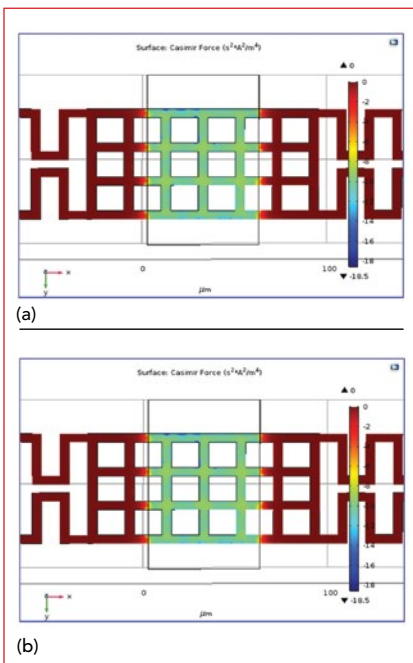

▲ **Fig. 15** Plots of measured Eigen frequency and pull-in-voltage of the primary shunt switches.

▲ **Fig. 16** Plots of measured Eigen frequency and pull-in-voltage of the secondary shunt switches.

SUMMARY

RF-MEMS switches can provide new solutions for the 5G and IoT applications in which reconfigurable broadband and frequency-agile devices, like high-order switching components, tunable filters, multi-state attenuators and phase shifters will be necessary to enable mmWave communications, small cells and advanced beamforming. [13-14]

As discussed in Part I and Part II of this series, reliability, packaging and integration with standard technologies, were the primary aspects that restricted the usage of MEMS devices in commercial markets.[15-18] Part III highlighted the research efforts that targeted the reliability concerns by exploiting Casimir effect in metamaterial inspired MEMS switch, resulting noteworthy improvement in switch characteristics for 5G and IoT applications.[19]

In this three-part article, the metamaterial structures described are split rings. However, other metamaterial structures can be used, provided those structures provide similar permittivity and permeability characteristics within the desired range of frequencies. For instance, a topology inspired Möbius transformation MTM (metamaterial) structures (meaning a structure that forms a continuous closed path that maps onto itself) can be considered advantageous for generating repulsive Casimir forces.[9] Although this series of articles described specific new configurations of MEMS switches, these are just some embodiments of designs that are merely illustrative of the principles and applications of the present invention.[1] It is therefore to be understood that numerous modifications can be made to these designs that utilize the same principals demonstrated here.■

References

1. Shiban Koul, Ajay Poddar, Ulrich Rohde, "Microelectromechanical Switch with Metamaterial Contacts," *US Patent Pub. No. 02161415A1*.
2. Astrid Lambrecht, "The Casimir Effect: a Force from Nothing," *Physics World September 2002*.
3. F. Intravaia and C. Henkel, *New Frontiers of Casimir Force*, Santa Fe, New Mexico, 2009.
4. U. Leonhardt and T. G. Philbin, "Quantum Levitation by Left-Handed Metamaterials," *New J. of Physics*, August 2007.
5. Mercado et. al, "A Mechanical Approach to Overcome RF MEMS Switch Stiction Problem," *ECTC 2003*.
6. Chaitanya Mahajan, "Design and Analysis of RF MEMS Switches (70 Ghz to 130 GHz), M. Tech dissertation, *CARE*, IIT Delhi, May 2018.
7. J. Sun, X. K. Hua and L. Gao, "Repulsive and Attractive Casimir Forces between Magnetodielectric Slabs," *Solid State Commun.*, Vol. 152, No. 17, September 2012, pp. 1666–1669.
8. V. Yannopapas and N. V. Vitanov, "First-Principles Study of Casimir Repulsion in Metamaterials," *Phys. Rev. Lett.*, Vol. 103, No. 12, September 2009, pp. 120401.
9. Ulrich Rohde, Ajay Poddar and Shiban Koul, "MTM: Casimir Effect and Gravity Wave Detection" *APMC 2016*.
10. Xudong Chen et. al," Robust Method to Retrieve the Constitutive Effective Parameters of Metamaterials," *Phy. Rev. E70*, 016608, July 2004.
11. S. Chaturvedi, S. Bhalke, M. Bhat K., G. Sai Saravanan, R. Muralidharan and Shiban K. Koul, "EM Simulation and Development of Wafer Level Micro-Packaging Technique for GaAs-based RFMEMS Switches," *Compound Semiconductor Manufacturing Techniques (CSMANTECH) Conference*, May 17-20, 2010, Portland, Ore., U.S., pp. 303-305.
12. S. Chaturvedi, "Modelling of Packages for MMICs and MEMS, Ph.D. Thesis, IIT Delhi under the supervision of Shiban K Koul," *CARE*, IIT Delhi, 2012.
13. L.-Y. Ma et al, "Comprehensive Study on RF-MEMS Switches Used for 5G Scenario," *IEEE Access*, Vol. 7, pp. 107506–22, 2019.
14. J. Iannacci et. al, "RF-MEMS Monolithic K and Ka Band Multi-State Phase Shifters as Building Blocks for 5G and Internet of Things (IoT) Applications," *MDPI Journal*, Sensors, 2020.
15. S. Dey, S. K. Koul, A. K. Poddar and U.L. Rohde, "RF MEMS Switches, Switching Networks and Phase Shifters for Microwave to Millimeter Wave Applications," *ISSS Journal of Micro and Smart Systems*, April 2020.
16. G.S. Karthikeya, S. K. Koul, A. K. Poddar and U.L. Rohde, "Ultra-compact Orthogonal Pattern Diversity Antenna Module for 5G Smartphones," *Microwave and Optical Technology Letters*, March 2020.
17. S. Dey, S. K. Koul, A. K. Poddar and U.L. Rohde, "Compact, Broadband, and Reliable Lateral MEMS Switching Networks for 5G Communications," *PIERS*, pp. 163–171, January 2019.
18. S. Dey, S. K. Koul, A. K. Poddar, U.L. Rohde, "Reliable and Compact 3- and 4-Bit Phase Shifters Using MEMS SP4T and SP8T Switches," *Journal of Micromechanical Systems*, pp. (99):1-12, January 2018.
19. A. K. Poddar, "Slow Wave Resonator Based Tunable Multi-Band Multi-Mode Injection-Locked Oscillator," *Dr.-Ing.-Habil Thesis*, BTU Cottbus, Germany, 2014.